JCTC Journal of Chemical Theory and Computation

ARTICLE

pubs.acs.org/JCTC

A Computational Study (TDDFT and RICC2) of the Electronic Spectra of Pyranoanthocyanins in the Gas Phase and Solution

Angelo Domenico Quartarolo and Nino Russo*

Dipartimento di Chimica and Centro di Calcolo ad Alte Prestazioni per Elaborazioni Parallele e Distribuite-Centro di Eccellenza MIUR, Università della Calabria, I-87030 Arcavacata di Rende, Italy

Supporting Information

ABSTRACT: The conformational structures and UV−vis absorption electronic spectra of a class of derived anthocyanin molecules (pyranoanthocyanins) have been investigated mainly by means of density functional (DFT) and time-dependent DFT methods. Pyranoanthocyanins are natural pigments present in aged wines and absorb at shorter wavelengths (around 500 nm) than the parent anthocyanin compounds, giving an orange-brown colored solution. The investigated molecules are derived from the reaction of glycosylated malvidin, peonidin, and petunidin with enolizable molecules (acetaldehyde and pyruvic acid) and vinyl derivatives. During wine storage, the concentration of pyranoanthocyanins increases with time, and analytical measurements (e.g., UV−vis spectroscopy) can characterize aged wines by color analysis. The prediction of absorption electronic spectra from TDDFT results, with the inclusion of water bulk solvation effects through the conductor-like polarizable continuum model, gives an absolute mean deviation from experimental absorption maxima of 0.1 eV and a good reproduction of the spectra line shape over the visible range of the spectrum. TDDFT calculated excitation energies agree with those obtained from *ab initio* multireference coupled cluster with the resolution of identity approximation (RICC2) methods, calculated at DFT gas-phase geometries.

1. INTRODUCTION

Anthocyanins are naturally occurring pigments present in the tissues of vascular plants, including leaves, flowers, fruits, and roots, and belong to the general class of flavonoids compounds.[1−4] They are based on the flavilium ion or 2-phenylchromenylium with the basic chemical structure, shown in Scheme 1, constituted by an aromatic ring (A) fused to an oxygen-containing heteroaromatic ring (C) and a third ring (B), which is connected to ring C through a carbon−carbon single bond.[5] The benzopyrilium ring (A and C fused rings) assumes a rigid planar conformation, while the substituted phenyl group (ring B) can freely rotate, giving rise to different conformational energy minima. Side R groups in Scheme 1 can be represented by hydrogen, hydroxyl, methoxy, glucoside, and its derivatives, and their possible combination gives a great number of different structures.[2] Depending upon the presence or not of the glycosyl moiety, anthocyanins are respectively named anthocyanin glycosides or anthocyanidin aglycons. They play an important biological role in plant metabolism, for example, in the pollination, reproduction, or photoprotection of the plants against high-energy UV solar radiation damage of plant cells.[6] This latter function is the basis of the antioxidant activity of anthocyanins to scavenge free radicals produced by metabolism and can also give benefits to human health for the prevention of different diseases like cardiovascular illnesses, diabetes, or tumors.[7−9] An important feature of anthocyanins is that they are responsible for fruit and flower colors, which differ according to the nature of the anthocyanin pigments present, since visible absorption maxima and intensity are strictly related to their molecular structures.[10−13] The color property of anthocyanins is also employed in the food industry, where they are used as vegetable colorants together with carotenoid pigments replacing synthetic dyes.[14]

The molecular stability to degradation of pure anthocyanin solutions depends on different factors such as the concentration, pH variation, molecular structure, storage temperature, light, complexation with metallic ions in solution, and oxygen.[11,15,16] The analysis of these factors can be helpful in the food industry for improving the stabilization of anthocyanins as food colorants. The anthocyanin solution concentration, the pH variation, and the presence of copigments and/or metallic ions also affect color properties. In solution, anthocyanins exist in different equilibrium forms depending on pH values. In strong acidic aqueous solutions (pH = 1−3), the predominant species present in solution is the flavilium cation (Scheme 1), which gives a strong red color. Increasing the pH between 2 and 4, the quinoidal species, formed after proton abstraction from the hydroxyl groups, are dominant with a bathochromic wavelength shift. At a pH between 5 and 6, after water hydrolysis, the colorless carbinol pseudobase and chalcone species appear in solution, while at alkaline pH, anthocyanins tend to degrade depending on the nature of the substituent R groups on the B ring. The larger the number of methoxy or hydroxyl groups on the B ring, the less stable the corresponding anthocyanidin is in neutral media. On the other hand, anthocyanin glycosides are more stable since the presence of the glycosyl moiety prevents the degradation reaction.[1,17] A class of anthocyanin-derived pigments or pyranoanthocyanins (Scheme 1), with different properties from anthocyanins, was detected in red wine filtrates by Cameira dos Santos et al. in 1996 and has attracted much attention in recent years for its possible use in characterizing aged wines.[18] Pyranoanthocyanins are more stable at different pH values with a

Received: December 23, 2010
Published: March 23, 2011

Scheme 1. Molecular Structures with Substituent (R) and Ring Labelling for Flavilium Cation (Upper Panel) and Investigated Pyranoanthocyanins

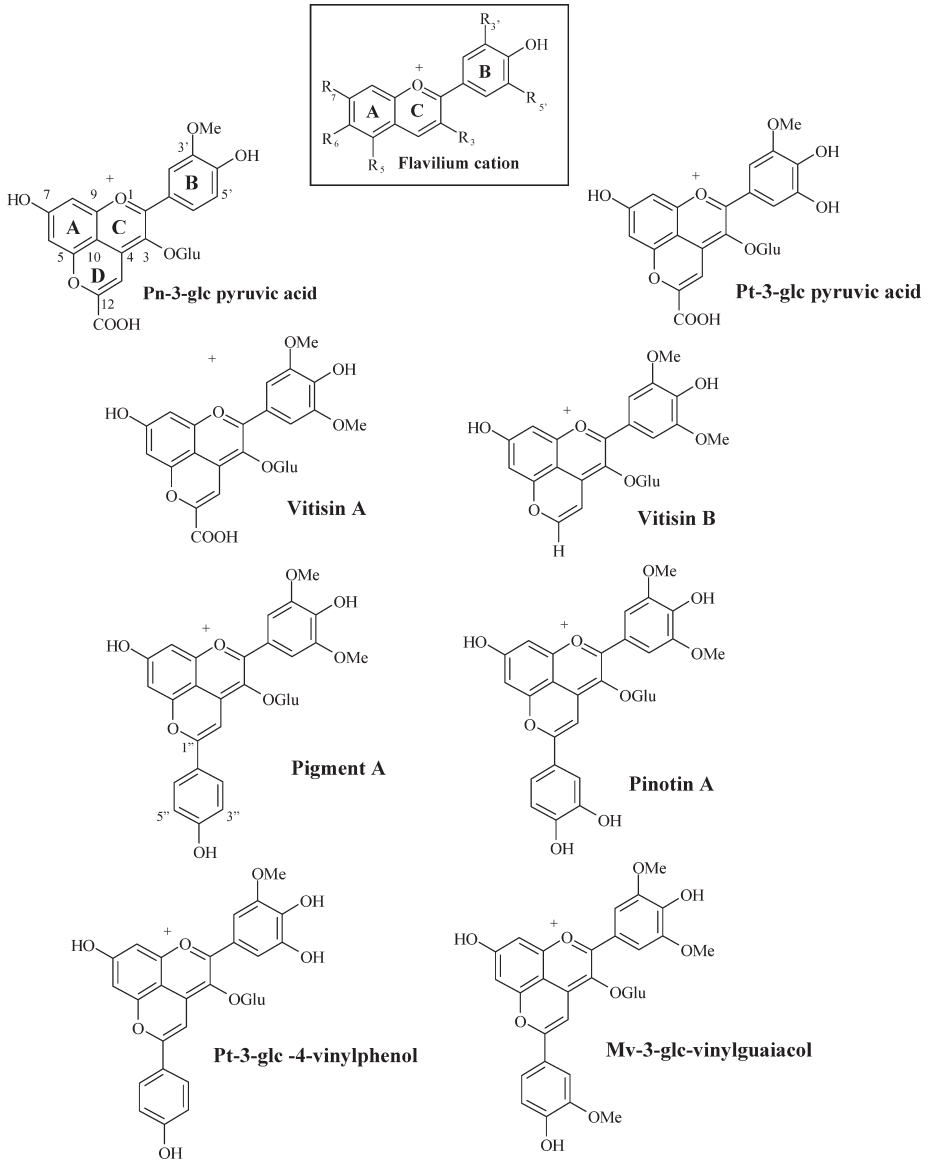

hypsochromic shift of the absorption wavelength maxima λ_{max}, in comparison with the anthocyanin monoglucosides, and that gives an orange-brown color to their solution.[19] These compounds are derived from the reaction of anthocyanins with low molecular weight molecules as flavonols, pyruvic acid, and 4-vinylphenol; the cyclization that takes place between the carbon at position 4 and the hydroxyl group at position 5 (Scheme 1) forms a fourth ring (ring D in Pe-3-glc pyruvic acid of Scheme 1) or pyran ring.[20,21] The stability of pyranoanthocyanins is due to the formation of the pyran ring that works as a protective group against the nucleophilic addition of water, avoiding the formation of the colorless carbinol pseudobase and decolorization by bisulphite (SO_2). The formation of pyranoanthocyanins in model solutions has been found to be fast and dependent on the initial concentrations of anthocyanins and the reaction partners (e.g., acetaldehyde, pyruvic acid, and other enolizable molecules) as well as on pH and temperature conditions.[22,23] Another important factor for their formation is the storage time; in fact, in red wines, although absent in the initial products, the concentration of pyranoanthocyanins increases with time.[24] The occurrence of pyranoanthocyanins was investigated and detected also in fermented and unfermented juices of black carrots, blood oranges, and strawberry fruits.[25−27] The identification methods for anthocyanins and pyranoanthocyanins are based on high-performance liquid chromatography combined with mass spectrometry and other spectroscopic techniques like nuclear magnetic resonance and UV−vis spectroscopy.[28−33] The latter is an important analytical tool giving both quantitative and qualitative information, like acid constant determinations, with low cost.[34,35] In recent years, theoretical studies, both *ab initio* and semiempirical, have also been done, in order to investigate different aspects of the chemistry of anthocyanins and pyranoantocyanins.[36−38] Density functional methods (DFT), for example, have been used to

predict the stability of charge transfer complexes between anthocyanins in the presence of copigment molecules (like hydroxycinnamic acids, e.g., gallic or caffeic acid)[39] or, in the case of pyranoanthocyanins, to study the reaction mechanisms responsible for the antioxidant activity.[40,41] Theoretical studies on UV−vis spectra of anthocyanins and pyranoanthocyanins have also been done by using semiempirical methods (e.g., ZINDO) or the time-dependent DFT approach (TDDFT).[42,44] In this paper, the electronic absorption spectra of pyranoanthocyanins, reported in Scheme 1, will be mainly investigated by the TDDFT methodology, which has become, in the past decade, a well assessed theoretical tool for the simulation of the electronic spectra (absorption, fluorescence, and phosphorescence) of medium and large organic and transition metal containing molecules.[45] The coupled cluster with approximate singles and doubles method and the resolution of identity approximation (RICC2), a correlated and size-consistent method, will also be applied to pyranoanthocyanins as an *ab initio* multiconfigurational reference approach.[46] The main purpose of this work is to theoretically characterize the electronic spectra and find a possible structure−property correlation for the pyranoanthocyanins in Scheme 1, together with a comparison of the theoretical results with available experimental electronic spectra.

2. COMPUTATIONAL METHODS

All calculations were carried out with the Turbomole software package on a Quad-Core AMD Opteron processor (2.7 CPU GHz with 62.9 GB memory).[47] Structures were preoptimized at the DFT theory level with the Becke−Perdew exchange-correlation functional (PBE)[48,49] and the resolution of identity approximation (RIDFT module)[50,51] avoiding the direct four-center integral calculation. The double-ζ-quality SV(P) and corresponding auxiliary basis sets, with polarization functions for C and O atoms, were adopted during this step.[52,53] The final structure optimizations were done with the PBE0 free-parameter hybrid functional,[54] which adds a fixed fraction (1/4) of the Hartree−Fock exact exchange energy to the PBE exchange-correlation functional,[55] and the SV(P) basis set. Optimized stationary points were characterized as energy minima by vibrational frequency calculations. An extensive basis set benchmark has been performed on Peonidin-3-glucoside pyruvic acid, in order to assess the basis set influence on the main excitation energy (experimental maximum absorption at 2.47 eV). The Ahlrichs double- [SV(P), SVP with polarization functions for hydrogens][52] and triple-ζ basis sets (TZVP)[56] give an excitation energy of 2.30 eV (539 nm), for both SV(P) and SVP basis sets, and 2.29 eV (540.5 nm) for the TZVP basis set. In the case of the SV(P) basis set, the addition of s and p diffuse functions for carbon and oxygen atoms yields a maximum absorption at 2.29 eV (541.5 nm). The use of correlation-consistent basis sets (cc-pVDZ and cc-pVTZ) developed by Dunning[57] gives values of 2.31 eV (535.8 nm) and 2.32 eV (534.5 nm), respectively. The maximum absorption difference, between the SV(P) and the more extended triple-ζ basis sets (TZVP and cc-pVTZ), is small and within 0.02 eV (10 nm). On the basis of these results, excitation energies were calculated on PBE0/SV(P) optimized structures by means of the TDDFT method at the same level of theory. This approach has been successfully applied for the prediction of UV−vis electronic spectra of organic and metal-transition containing systems, yielding an error within 0.3−0.4 eV.[58−61] Bulk solvent effects were taken into account both on geometries and excitation energies by means of the conductor-like polarizable continuum model (CPCM)[62,63] by setting the dielectric constant ε to 78.39 in order to simulate an aqueous medium, since pyranoanthocyanins are water-soluble. For the cavity construction on each atom, default parameters (solvent radius and optimized atomic radii) as defined in the COSMO module were chosen. The band shapes of the electronic spectra were reproduced, using the SWizard program,[64] by a sum of Gaussian functions centered on each excitation energy according to the formula

$$\varepsilon(\omega) = 2.174 \times 10^8 \sum_I \frac{f_I}{\Delta_{1/2}} \exp\left(-2.733 \frac{(\omega - \omega_I)^2}{\Delta_{1/2}}\right) \quad (1)$$

where molar absorbance ε is given in M^{-1} cm^{-1} units and ω_I and f_I are, respectively, the excitation energies and oscillator strengths for each allowed electronic transition. The sum in eq 1 is such that the total integrated intensity under the absorption profile is equal to the sum of the oscillator strengths f_I. A constant half-height bandwidth $\Delta_{1/2}$ of 0.3 eV has been chosen in order to match the corresponding experimental spectra. The lowest 30 excitation energies were included in the spectra simulation. For a theoretical comparison with TDDFT excitation energies, also the RICC2 model has been applied at gas-phase optimized DFT geometries, with the frozen orbital space option.[65] Moreover, in order to make computationally feasible the RICC2 calculations, the SV(P) basis set has been employed through all of the calculations. In fact, as found for the TDDFT basis set benchmark, the use of larger basis sets results in little improvment in the accuracy of the main excitation energy. For the Pn-3-glc pyruvic acid derivative, the use of TZVP and correlation-consistent basis sets (cc-pVDZ, cc-pVTZ, and aug-cc-pVDZ) yields the main excitation energy at 2.33 eV [SV(P), SVP, cc-pVDZ] and 2.37 eV (TZVP, cc-pVTZ, and aug-cc-pVDZ). Optimized Cartesian coordinates for all molecular structures (in water) are included in the Supporting Information (pp S2−S13).

3. RESULTS AND DISCUSSION

3.1. Conformational Structures. The investigated pyranoanthocyanins reported in Scheme 1 are structurally derived from the condensation reaction of organic molecules with three kinds of glycosylated anthocyanins: malvidin- ($R_{3'}$ = $R_{5'}$ = OCH_3), peonidin- ($R_{3'}$ = OCH_3, $R_{5'}$ = H), and petunidin-3-glucosides ($R_{3'}$ = OCH_3, $R_{5'}$ = OH), abbreviated in the text respectively as Mv-, Pe-, and Pt-3-glc (see Scheme 1). When the reaction occurs between pyruvic acid and Pn-, Pt-, and Mv-3-glc, the products are the two pyruvic derivatives and Vitisin A, whereas the reaction of Mv-3-glc with acetaldehyde gives the pyranoanthocyanin derivative named Vitisin B. The main structural difference among them is represented by the side ring C substituent groups at positions 3′ and 5′ and in the case of Vitisin B by the presence of the hydrogen atom at position 12′ in place of the carboxylic group. A different structure modification can be obtained from the reaction of anthocyanins with vinylphenol, vinylcathecol, and vinylguaiacol, which causes an elongation of the molecular system at position 12′. The reaction between Mv- and Pt-3-glc with 4-vinylphenol gives, respectively, Pigment A and Pt-3-glucoside-4-vinylphenol derivatives, while Pinotin A and Mv-3-glc-vinylguaiacol come from the reaction between Mv-3-glc and vinylcathecol and vinylguaiacol molecules, respectively

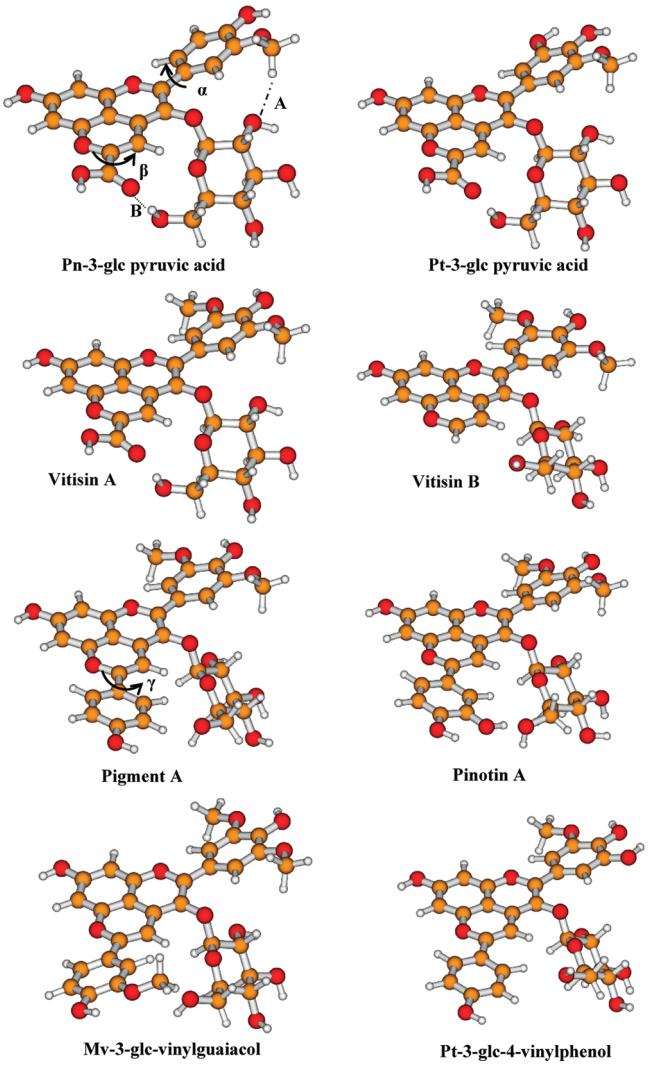

Figure 1. Pyranoanthocyanin global minimum structures.

(Scheme 1). For all studied pyranoanthocyanins, only the red flavilium cation was taken into account for molecular properties calculations. In fact, pyranoanthocyanins are less sensitive to pH increases with respect to anthocyanins, so for example at wine pH (about 3.6), the dominant contributing molecular structure, in solution equilibrium, can be considered the flavilium cation. Like anthocyanins, pyranoanthocyanins can coexist in solution in different conformational structures because of the free rotation around carbon−carbon single bonds. In particular, three main conformational degrees can be identified: (a) the rotation of ring B around the carbon−carbon single bond that connects it to ring C (torsional angle α in Figure 1), (b) the rotation around the bond connecting the carbon atom at position 12 of Scheme 1 to carboxylic (angle β in Pn-3-, Pt-3-glc derivatives and Vitisin B in Figure 1) and substituted phenyl groups (angle γ in Pigment A and the analogous parameter in vinyl derivatives in Figure 1), and (c) the free rotation of hydroxyl and methoxy groups attached at different ring positions (A−D rings in Scheme 1) and a sugar moiety, which can form intramolecular stabilizing hydrogen bonds. The sugar moiety has been chosen as in the β-D-glucopyranose conformation, having the hydroxymethyl group oriented in the equatorial (gauche) position, which is the most abundant anomeric form in water.[66,67] The optimized structures of the most stable conformers for each pyranoanthocyanin are shown in Figure 1, while that of the less stable conformers and the relative energy (kcal/mol) with respect to the most stable conformer are reported in the Supporting Information (pp S14−S16).

The energetic differences are within 10 kcal/mol and are in some cases negligible. The driving force that stabilizes the structures in Figure 1, or in general each conformer to the less stable one, can be attributed to the number of hydrogen bonds formed. The value of the dihedral angle α is due to a delicate balance between the degree of electronic delocalization (through ring B and the rest of the molecule) and the nature of the interactions of ring B hydrogens with the glycosyl group. For malvidin-based pyranoanthocyanins (e.g., Vitisin-A and Pigment A), the methyl groups on ring C are oriented in opposite directions, so the main conformational variable is represented by the group orientation at position 12′ (carboxylic or vinyl derivatives). Pyruvic acid adducts and Vitisin-B have the C ring rotated by about 20° (dihedral angle α in Figure 1) and the carboxylic group rotated by about 15−17° (dihedral angle β in part A). The oxygen atom forms a hydrogen bond with a length between 1.8 and 1.9 Å (interaction B in Figure 1). For Vitisin B, the absence of the carboxylic group reduces the sterical interaction between the sugar moiety and ring C, and as a consequence, there is a decrease in angle α (about 9°). A weaker interaction (about 2.4 Å) exists between the methyl group oxygen on the C ring and the sugar hydroxyl group (A interaction in Figure 1). For vinyl derivatives (Pigment A, Pinotin A, Mv-3-glc, and Pt-3-glc derivatives), angle α is similar to that found for pyruvic and acetaldehyde adducts, and it ranges between 16 and 20°. The torsional angle γ (see Pigment A and other vinyl derivatives in Figure 1) that describes the mutual rotation between ring D and substituted phenyl is small for Pigment A and Pt-3-glc-4-vinylphenol (respectively about 4 and 6°). For these two molecules, the phenyl group has one hydroxyl substituent at the *para* position that does not interact, through a hydrogen bond, with the glycoside moiety. The most stable conformers of Pinotin A and Mv-3-glc-4-vinylguaiacol are characterized by a dihedral angle γ of 12 and 19°, respectively. The increased γ rotation is mainly due to the formation of hydrogen bonding between the methoxy (for Pinotin A) and hydroxyl (for Mv-3-glc-4-vinylguaiacol) substituents at position 3′′ and the $-CH_2OH$ (hydroxymethyl) group on the glycoside moiety.

3.2. Electronic Spectra. The TDDFT results, regarding *in vacuo* and water (CPCM model) excitation energies (in eV and nm units), transition configurations, and oscillator strengths, have been collected in Tables 1 and 2. In particular, in Table 1, pyruvic and acetaldehyde anthocyanin derivatives are grouped together, whereas in Table 2, the results obtained for the vinyl derivatives that possess a structure elongation at position 12 of ring D (see Scheme 1) are shown. For all three pyruvic and acetaldehyde adducts in Table 1, the most intense signal is given by a HOMO to LUMO transition ($\pi \rightarrow \pi^*$ with charge transfer character, see Figure 2), with oscillator strengths f between about 0.3 and 0.4. For Vitisin A, in the visible region, there are two *in vacuo* excitation energies with comparable strengths: the first at 573 nm (f = 0.2347) and the second at 506 nm (f = 0.2834). In this case, the convoluted simulated spectrum gives the maximum absorption band centered at 529 nm. In the same way, for Vitisin B, the maximum absorption wavelength (λ_{max}) is at 488 nm, which is lower by 10 nm than the first excitation energy (2.49 eV,

Table 1. Calculated Excitation Energies ΔE (eV, nm), Main Configuration (Percentage Contribution in Parentheses), and Oscillator Strengths f (*in vacuo* and Water), for Peonidin- and Petunidin-3-Glucoside Pyruvic Acids (Pn-3-glc and Pt-3-glc der.), Vitisin A, and Vitisin B[a]

		TDDFT[b]					
		vacuum			c-pcm (water)		
molecule	state	ΔE (eV,nm)	f	configuration	ΔE (eV,nm)	f	exptl.
Pn-3-glc der.	1 ^{1}A	2.30, 539	0.2971	H → L (94.5)	2.45, 506	0.3063	2.47, 503[c]
	2 ^{1}A	2.81, 442	0.1970	H-1 → L (93.8)	2.85, 435	0.1235	
	3 ^{1}A	2.89, 429	0.0350	H-2 → L (97.3)	3.16, 392	0.0654	
Pt-3-glc der.	1 ^{1}A	2.27, 547	0.0084	H-1 → L (96.6)	2.47, 503	0.4195	2.45, 507[c]
	2 ^{1}A	2.35, 527	0.4737	H→ L (95.5)	2.52, 492	0.0486	
	3 ^{1}A	2.87, 432	0.0116	H-2 → L (86.4)	2.95, 421	0.0138	
Vitisin A	1 ^{1}A	2.16, 573	0.2347	H → L (78.3)	2.40, 518	0.3892	2.45, 507 [c];
				H-1 → L (20.6)			2.44, 509[d]
	2 ^{1}A	2.45, 506	0.2834	H-1 → L (78.3)	2.58, 480	0.0802	
				H → L (19.9)			
	3 ^{1}A	2.87, 432	0.0069	H-2 → L (98.0)	2.95, 420	0.0155	
Vitisin B	1 ^{1}A	2.49, 498	0.3616	H → L (80.3)	2.71, 458	0.5473	2.53, 491[e]
				H-1 → L (18.2)			
	2 ^{1}A	2.72, 456	0.2660	H-1 → L (81.8)	2.93, 423	0.0337	
				H → L (17.5)			
	3 ^{1}A	3.24, 383	0.0112	H-2 → L (94.7)	3.22, 385	0.0072	
MAD[f]		0.08			0.06		

[a] Experimental absorption maxima (eV, nm) are also given for comparison. [b] TD-PBE0/SV(P)//PBE0/SV(P) level of theory. [c] See ref 30. [d] See ref 31. [e] See ref 33. [f] Absolute mean deviation MAD (eV) for the maximum absorption band *in vacuo* and water (CPCM model).

Table 2. Calculated Excitation Energies ΔE (eV, nm), Main Configuration (Percentage Contribution in Parentheses), and Oscillator Strengths f (*in vacuo* and water), for Pigment A, Pinotin A, Mv-3-glc-vinylguaiacol, and Pt-3-glc-4-vinylphenol[a]

		TDDFT[b]					
		vacuum			c-pcm (water)		
molecule	state	ΔE (eV, nm)	f	configuration	ΔE (eV, nm)	f	exptl.
Pigment A	1 ^{1}A	2.42, 513	0.7028	H→L (97.5)	2.60, 477	0.7512	2.47, 503;[c, d]
							2.46, 504[e]
	2 ^{1}A	2.75, 452	0.0976	H-1→L (92.7)	2.98, 417	0.0385	
	3 ^{1}A	3.07, 403	0.3578	H-1→L (92.7)	3.10, 400	0.2467	
				H-2→L (87.8)			
Pinotin A	1 ^{1}A	2.44, 509	0.8389	H→L(98.4)	2.63, 471	0.8232	2.42, 512;[c]
							2.44, 509[e]
	2 ^{1}A	2.73, 455	0.1262	H-1→L (87.3)	2.85, 436	0.0722	
	3 ^{1}A	2.84, 436	0.0291	H-2→L (89.2)	3.15, 393	0.0221	
Mv-3-glc- vinylguaiacol	1 ^{1}A	2.41, 514	0.8119	H→L (97.7)	2.58, 480	0.8358	2.42, 512[c]
	2 ^{1}A	2.73, 455	0.1492	H-1→L (57.9)	2.87, 433	0.1184	
				H-2→L (40.4)			
	3 ^{1}A	2.82, 439	0.0636	H-2→L (57.4)	2.98, 416	0.0098	
				H-1→L (38.9)			
Pt-glc-4-vinylphenol	1 ^{1}A	2.52, 492	0.7310	H→L (95.4)	2.65, 467	0.7964	2.47, 503[c]
	2 ^{1}A	2.71, 458	0.1245	H-1→L (94.2)	2.93, 423	0.0109	
	3 ^{1}A	3.08, 402	0.2923	H-2→L (92.4)	3.11, 399	0.2396	
MAD[f]		0.005			0.17		

[a] Experimental absorption maxima (eV, nm) are also given for comparison. [b] TD-PBE0/SV(P)//PBE0/SV(P) level of theory. [c] See ref 30. [d] See ref 31. [e] See ref 33. [f] Absolute mean deviation MAD (eV) for the maximum absorption band *in vacuo* and water (CPCM model).

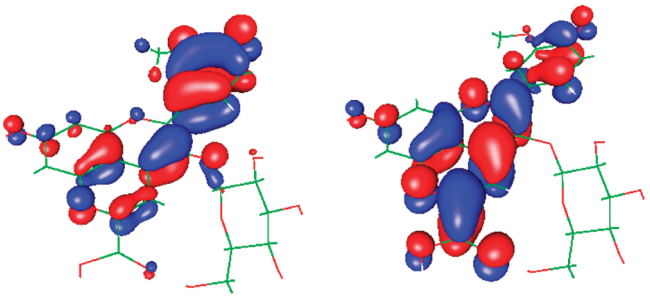

Figure 2. Isodensity molecular orbital plots (isodensity value of 0.03 au) of the HOMO and LUMO for the Pn-3-glc pyruvic acid derivative.

498 nm). For the other two molecules in Table 1 (Pn- and Pt-3-glc pyruvic adducts), the absorption maxima can be identified by their most intense transition (respectively at 539 and 527 nm). The inclusion of bulk solvation effects, through the CPCM model, lowers the absorption maxima and slightly intensifies the transition strengths, giving a better agreement with the experimental λ_{max}. Moreover, for Vitisin-type molecules, the second excitation energies, as obtained from gas-phase calculations, become less intense ($f \sim 0.03-0.08$), and the main electronic band is mainly described by the first excitation energy. For *in vacuo* and water solution calculations, the absorption maxima roughly correlate with the HOMO−LUMO DFT energy gap ($E_{H\rightarrow L}$). For example, for Vitisin-A, λ_{max} is slightly greater (about 15 nm) than those of the Pn- and Pt-3-glc pyruvic derivatives, and its $E_{H\rightarrow L}$ is decreased. In a similar way, Vitisin-B shows the lowest absorption maximum, among the compounds in Table 1, and the greatest $E_{H\rightarrow L}$ value (in water 3.06 eV). Frontier molecular orbital energies (*in vacuo* and water) for all of the investigated compounds are reported in the Supporting Information (pp S17−S18).

The calculated λ_{max} for pyruvic adducts does not strictly follow the experimental trend. The reason could be that the experimental values, as reported in Table 1, cover a small wavelength range (503−507 nm), while the TDDFT error, as found also for other classes of organic molecules, is generally within 0.3 eV or, in wavelength units, 1 or 2 orders of magnitude greater than the experimental difference.[56] The only case in which we can make a clear correlation between wavelength absorption maxima and molecular structure is Vitisin-B. This molecule, unlike pyruvic adducts, lacks the carboxylic group at position 12 of ring D that increases the electronic delocalization and consequently the molecule λ_{max}. For Vitisin B, the calculated λ_{max} decreases with respect to the other pyruvic acid adducts in agreement with the experimental trend. A rational explanation for the λ_{max} bathochromic shift of pyruvic acid derivatives with respect to Vitisin B can be derived from the energy and wave function analysis of the frontier molecular orbitals. The decreasing of the HOMO−LUMO energy gap ΔE_{H-L} for Pn-3- and Pt-3-glc pyruvic acid adducts and Vitisin-A (gas-phase ΔE_{H-L}= 2.69, 2.63, and 2.50 eV, see Table S1 in the Supporting Information) in comparison to that of Vitisin-B (ΔE_{H-L} = 2.79 eV) is due to a greater LUMO energy stabilization. For example, the gas-phase HOMO's molecular energy difference between Pn-3-glc pyruvic acid and Vitisin-B is 0.43 eV (in water 0.22 eV) and lower than the LUMO's corresponding value of 0.53 eV (in water 0.39 eV). Similar results are found for Pt-3-glc pyruvic acid adducts and Vitisin-A in comparison to Vitisin-B with a better LUMO energy stabilization. The molecular orbital composition analysis can help in the identification of which molecular structural factors cause the LUMO energy stabilization. For that purpose, the Mulliken electron population analysis procedure was followed for calculating the percentage weight of each atomic orbital to the HOMO and LUMO DFT orbitals.[68,69] The molecular structures of Vitisin-B and pyruvic acid derivatives have been considered as composed by four main molecular fragments: the central molecular core (fused A, C, and D rings), ring B, glycosyl, and, in the case of pyruvic acid derivatives, carboxylic groups. In this way, the electron density is partitioned according to the molecular fragment weight composition. The central fused ring (A, C, and D) fragment accounts for about 20% of the total electron density in the HOMO wave function composition. The most important percentage contribution comes from ring B (77−80), while the glycosyl and the carboxylic groups make a negligible contribution. On the other hand, for the LUMO orbital composition, ring B contributes 15−21% and fused rings A, C, and D 15−17%, and an important contribution is derived from the carboxylic group (9%), which is absent in the case of the Vitisin-B molecule. These results can explain the important role of carboxylic substituent groups in the LUMO energy stabilization and consequently the wavelength bathochromic shift in pyruvic acid derivatives with respect to Vitisin-B.

The influence of the conformational equilibria on the UV−vis spectra has been analyzed for the case of Pn-3-glc pyruvic derivative in the gas phase. The rotation around the dihedral angle α (see Figure 1) for that compound can give rise to another minima conformer (see Supporting Information, p S14) with a small energy difference in comparison to the more stable structure, shown in Figure 1 (ΔE = 1.1 kcal/mol). Neglecting in a first approximation the presence of other conformers, and applying the Boltzmann distribution formula at room temperature to the two conformers, we find that the resulting statistically weighted λ_{max} over the relative populations is about 536 nm. This value is almost identical to the *in vacuo* value of 539 nm (see Table 1). In a water solution, the energetic difference between the two conformers is lower (0.02 kcal/mol). Also in this case, the weighted λ_{max} (502 nm) is very close to the corresponding value calculated for the most stable conformer (λ_{max} = 506 nm). For that reason, the calculation of the electronic spectrum of the most stable conformer has been assumed as a valid approximation for the spectra of the molecule weighted in all possible energy minima conformations. The mean absolute deviations (MAD) for the most intense transition *in vacuo* and in a water solution, as extrapolated from the spectra simulation, are respectively 0.08 and 0.06 eV, showing an overall good agreement between experimental and calculated excitation energy in the visible region. In particular, the inclusion of solvent effects on wavelength maxima improves the quality of the results. The simulated electronic spectra in a water medium, for all compounds in Table 1, are shown in Figure 3 (left part) along with the experimental spectrum of Vitisin A that consists of an intense band in the visible region and other bands in the ultraviolet (UV) part of the spectrum. The calculated line shape of the spectrum also reproduces qualitatively the minor UV peaks (λ < 400 nm).

For the vinyl derivatives reported in Table 2, the experimental wavelength maxima range between 503 nm (Pigment A and Pt-3-glc-vinylphenol) and 512 nm (Mv-3-glc-vinylguaicol), while *in vacuo* calculated values are between 509 (Pinotin A) and 520 nm (Pt-3-glc-vinylphenol). In solution, the theoretical λ_{max} values are lowered and range between 471 and 486 nm. The MAD for this group of compounds, calculated for the *in vacuo* most intense

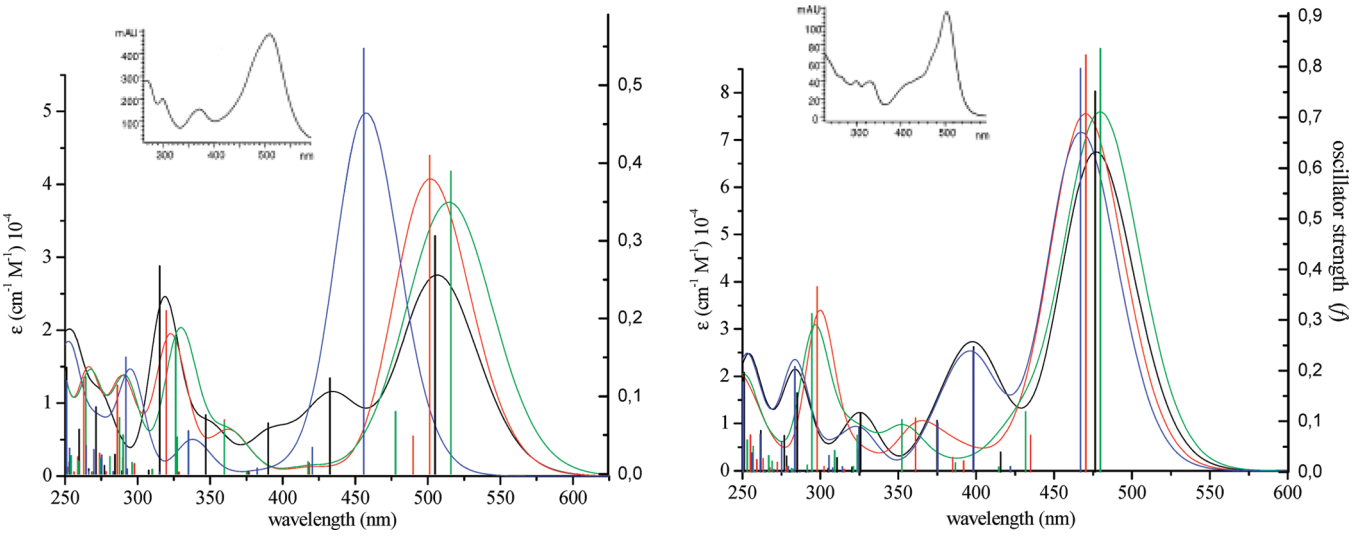

Figure 3. Simulated convoluted and stick electronic spectra in water of studied pyranoanthocyanins in Scheme 1 (absorption wavelength vs oscillator strength and molar absorptivity). On the left: Pn-3-glc pyruvic acid (black), Pt-3-glc pyruvic acid (red), Vitisin-A (green), and Vitisin-B (blue). On the right: Pigment A (black), Pinotin A (red), Mv-3-glc-vinylguaiacol (green), and Pt-3-glc-4-vinylphenol (blue). Experimental spectra of Vitisin-A (upper left part) and pigment A (upper right part) as taken from ref 30 are also reproduced.

Table 3. Calculated (RICC2) Excitation Energies ΔE (eV, nm), Main Configuration (Percentage Contribution in Parentheses), Singles Excitation Contribution T_1 (%), and Oscillator Strengths f for Peonidin-and Petunidin-3-Glucoside Pyruvic Acids (Pn-3-glc and Pt-3-glc der.), Vitisin A, and Vitisin B[a]

		RICC2[b]				
molecule	state	ΔE (eV, nm)	configuration	f	T_1	exptl.
Pn-3-glc der.	1 ^{1}A	2.37, 524.1	H→L (93.8)	0.6704	85.7	2.47, 503[c]
	2 ^{1}A	2.97, 417.6	H-1→L (65.9) H-2→L (28.1)	0.0946	86.6	
	3 ^{1}A	3.34, 371.3	H-2→L (64.3) H-1→L (23.4)	0.0683	86.0	
Pt-3-glc der.	1 ^{1}A	2.33, 533.1	H→L (93.4)	0.7526	86.2	2.45, 507[c]
	2 ^{1}A	2.64, 469.4	H-1→L (91.9)	0.1970	85.7	
	3 ^{1}A	3.05, 406.2	H-2→L (91.9)	0.0196	86.0	
Vitisin A	1 ^{1}A	2.15, 575.6	H→L (92.4)	0.7029	84.7	2.43, 511[d]
	2 ^{1}A	2.67, 464.2	H-1→L (89.8)	0.1174	85.5	
	3 ^{1}A	3.10, 399.8	H-2→L (91.7)	0.0178	86.4	
Vitisin B	1 ^{1}A	2.36, 524.6	H→L (94.1)	0.8054	85.4	2.53, 491[e]
	2 ^{1}A	2.93, 423.2	H-1→L (90.1)	0.0602	85.9	
	3 ^{1}A	3.26, 380.6	H-2→L (90.3)	0.0065	86.4	
MAD[f]						0.17

[a] Experimental absorption maxima (eV, nm) are also given for comparison. [b] RICC2/SV(P)//PBE(0)/SV(P) level of theory. [c] See ref 30. [d] See ref 31. [e] See ref 33. [f] Absolute mean deviation MAD (eV) for the *in vacuo* maximum absorption band.

excitation energy is 0.005 eV, whereas in a water solution the deviation is higher (0.17 eV). In Figure 2 (upper right part) is shown the experimental spectrum of Pigment A, which, apart from the main peak at 503 nm, has a broad minor peak centered at 423 nm. This electronic band corresponds to the third calculated excitation energy at 400 nm (f = 0.2467), which in the convoluted spectrum in Figure 2 is centered at 397 nm, showing good agreement with the experimental band. The final MAD for the eight pyranoanthocyanins is 0.04 eV *in vacuo* and 0.11 eV in water. The results obtained from *in vacuo* RICC2 calculations are reported in Tables 3 and 4. In addition to the TDDFT data types given in Tables 1 and 2 (e.g., excitation energies, configurations, and oscillator strengths), the percentage contribution of singles substitution (T_1) is also indicated, which gives the quality of the RICC2 excitation energies, in comparison to a full configuration interaction treatment. In this case, T_1 values are all between 84% and 87%; this means that electronic transitions have a small double character contribution. For pyruvic and acetaldehyde derivatives (Table 3), the experimental wavelength maxima increasing order (from Pn-3-glc to Vitisin B) is qualitatively reproduced with an absolute mean deviation of 0.17 eV, which is greater than that found for the vinyl derivatives (0.07 eV). The MAD for all investigated systems as obtained from RICC2 gives a value of 0.12 eV that is comparable to the corresponding values for water solution TDDFT calculations.

Table 4. Calculated RICC2 Excitation Energies ΔE (eV, nm), Main Configuration (Percentage Contribution in Parentheses), Singles Excitation Contribution T_1 (%) and Oscillator Strengths f for Pigment A, Pinotin A, Mv-3-glc-vinylguaiacol, Pt-3-glc-4-vinylphenol[a]

		RICC2[b]				
molecule	state	ΔE (eV, nm)	configuration	f	T_1	exptl.[c]
Pigment A	1 ^{1}A	2.33, 531.2	H→L (94.4)	1.0553	85.4	2.47, 503;[c,d] 2.46, 504[e]
	2 ^{1}A	3.00, 414.0	H-1→L (55.9) H-2→L (29.6) H-3→L (7.4)	0.1775	85.8	
	3 ^{1}A	3.16, 392.7	H-2→L (61.8) H-1→L (26.2) H-3→L (4.1)	0.2116	85.9	
Pinotin A	1 ^{1}A	2.36, 525.2	H→L (94.0)	1.1884	85.6	2.42, 512;[c] 2.44, 509[e]
	2 ^{1}A	2.84, 436.9	H-1→L (92.8)	0.2552	85.3	
	3 ^{1}A	3.13, 395.8	H-2→L (81.8)	0.0182	85.4	
Mv-3-Glu-4-vinylguaiacol	1 ^{1}A	2.31, 535.7	H→L (94.3)	1.1449	85.4	2.42, 512[c]
	2 ^{1}A	2.86, 434.1	H-1→L (90.1)	0.2801	85.3	
	3 ^{1}A	3.06, 405.2	H-2→L (83.8)	0.0277	85.3	
Pt-Glu-4-vinylphenol	1 ^{1}A	2.50, 495.8	H→L (93.4)	1.1356	86.2	2.47, 503[c]
	2 ^{1}A	3.04, 408.3	H-1→L (68.8) H-2→L (19.0) H-3→L (5.1)	0.0720	85.7	
	3 ^{1}A	3.17, 391.5	H-2→L (72.6) H-1→L (17.1)	0.2157	86.0	
MAD[f]						0.07

[a] Experimental maxima wavelengths (eV, nm) are also given for comparison. [b] RICC2/SV(P)//PBE(0)/SV(P) level of theory. [c] See ref 30. [d] See ref 31. [e] See ref 33. [f] Absolute mean deviation MAD (eV) for the *in vacuo* maximum absorption band.

4. CONCLUSIONS

The theoretical electronic spectra of a group of anthocyanin-derived pigments have been computed by means of TDDFT and RICC2 methods. A preliminary conformational analysis was performed over all of the investigated pyranoanthocyanins in order to identify the most stable conformer within each. As for anthocyanins, the simultaneous rotation of ring C and substituents at position 12′ of ring D (Figure 1) around carbon−carbon single bonds gives rise to several energy minima. Steric and intramolecular hydrogen bond factors can rationalize the relative energy stability of each conformer, whose difference is within 10 kcal/mol of the most stable conformer taken as an absolute energy minimum reference.

Calculated TDDFT excitation energies both *in vacuo* and in a water solution (CPCM model) showed mean absolute deviations of 0.04 and 0.11 eV, respectively. The latter value is comparable with that of the more refined RICC2 method, which gives MAD equal to 0.12 eV. Wavelength maxima absorption shifts due to molecular structural differences have been theoretically predicted between piruvic and acetaldehyde acid adducts. In particular, the presence of the electron-withdrawing carboxylic group attached on ring D for Pn-, Pt-, and Mv-3-glc derivatives causes, in accordance with the experimental findings, a bathochromic wavelength shift with respect to Vitisin B, due to the lowering of the HOMO−LUMO energy gap. However, the small differences between pyranoanthocyanin experimental wavelength maxima do not allow one to correctly predict, for all the sets of molecules at the TDDFT level, the λ_{max} experimental changes according to the molecular structure differences. The Gaussian convolution of the excitation energies and oscillator strengths, for the solution simulation of the electronic spectra profile over the UV−visible part of the spectrum, gives a qualitatively good agreement with the experimental absorption line shape profiles as shown in Figure 3 for the cases of Vitisin-A and Mv-3-glv vinylguaiacol.

■ ASSOCIATED CONTENT

Supporting Information. Optimized Cartesian coordinates in water for pyranoanthocyanins reported in Figure 1, optimized structures for other possible conformers with absolute and relative energies, frontier molecular orbital energies. This material is available free of charge via the Internet at http://pubs.acs.org.

■ AUTHOR INFORMATION

Corresponding Author

*Tel.: +39-0984-492048. Fax: +39-0984-492044. E-mail: nrusso@unical.it.

■ ACKNOWLEDGMENT

The University of Calabria, the Food Science and Engineering Interdepartmental Center of the University of Calabria, and L.I.P.A.C., Calabrian Laboratory of Food Process Engineering (Regione Calabria APQ - Ricerca Scientifica e Innovazione Tecnologica I atto integrativo, Azione 2 laboratori pubblici di ricerca mission oriented interfiliera, and Azione 3 sostegno alla domanda di innovazione nel settore agroalimentare) are gratefully acknowledged.

■ REFERENCES

(1) Castañeda-Ovando, A.; Pacheco-Hernández, M.; Páez-Hernández, E.; Rodríguez, J. A.; Galán-Vidal, C. A. *Food Chem.* **2009**, *113*, 859–871.

(2) Yoshida, K; Mori, M.; Kondo, T. *Nat. Prod. Rep.* **2009**, *26*, 884–915.

(3) Veitch, N. C.; Grayer, R. J. *Nat. Prod. Rep.* **2008**, *25*, 555–611.

(4) Andersen, Ø. M.; Jordheim, M. In *Flavonoids: Chemistry, Biochemistry and Applications*; Andersen, Ø. M., Markham, K. R., Eds.; Taylor & Francis Group: Oxford, U. K., 2009; Chapter 10, pp 471−553.

(5) Pauling, L. *Fortschr. Chem. Org. Nat.* **1939**, *3*, 203–235.

(6) Hatier, J-H. B.; Gould, K. S. In *Anthocyanins: biosynthesis, functions, and applications*; Gould, K., Davies, K., Winefield, C., Eds.; Springer Science: New York, 2009; Chapter 1, pp 1−12.
(7) Kähkönen, M. P.; Heinonen, M. *J. Agric. Food Chem.* **2003**, *51*, 628–633.
(8) Halliwell, B. *J. Sci. Food Agric.* **2006**, *86*, 1992–1995.
(9) Record, I. R.; Dreosti, I. E.; McInerney, J. K. *Br. J. Nutr.* **2001**, *85*, 459–464.
(10) Fossen, T.; Cabrita, L.; Andersen, Ø. M. *Food Chem.* **1998**, *63*, 435–440.
(11) Cabrita, L.; Fossen, T.; Andersen, Ø. M. *Food Chem.* **2000**, *68*, 101–107.
(12) Wrolstad, R. E.; Durst, R. W.; Lee, J. *Trends Food Sci. Technol.* **2006**, *16*, 423–428.
(13) Heredia, F. J.; Francia-Aricha, E. M.; Rivas-Gonzalo, J. C.; Vicario, I. M.; Santos-Buelgab, C. *Food Chem.* **1998**, *63*, 491–498.
(14) Mateus, N.; de Freitas, V. In *Anthocyanins: biosynthesis, functions, and applications*; Gould, K., Davies, K., Winefield, C., Eds.; Springer Science: New York; 2009; Chapter 9, pp 283−298.
(15) Borkowsky, T.; Szymusiak, H.; Gliszczynska-Swiglo, A.; Tyrakowska, B. *Food Res. Int.* **2005**, *38*, 1031–1037.
(16) Fuyuki, I.; Tanaka, N.; Katsuki, A.; Fujii, T. *J. Photochem. Photobiol., A* **2002**, *150*, 153–157.
(17) Fleschhut, J.; Kratzer, F.; Rechkemmer, G.; Kulling, S. E. *Eur. J. Nutr.* **2006**, *45*, 7–18.
(18) Cameira dos Santos, P. J.; Brillouet, J. M.; Cheynier, V.; Moutounet, M. *J. Sci. Food Agric.* **1996**, *70*, 204–208.
(19) Rentzsch, M.; Schwarz, M.; Winterhalter, P. *Trends Food Sci. Technol.* **2007**, *18*, 526–534.
(20) Bakker, J.; Timberlake, C. F. *J. Agric. Food Chem.* **1997**, *45*, 35–43.
(21) Fulcrand, H.; Benabdeljalil, C.; Rigaud, J.; Cheynier, V.; Moutounet, M. *Phytochemistry* **1998**, *47*, 1401–1407.
(22) Romero, C.; Bakker, J. *J. Agric. Food Chem.* **1999**, *47*, 3130–3139.
(23) Schwarz, M.; Wabnitz, T. C.; Winterhalter, P. *J. Agric. Food Chem.* **2003**, *51*, 3682–3687.
(24) Schwarz, M.; Hofmann, G.; Winterhalter, P. *J. Agric. Food Chem.* **2004**, *52*, 498–504.
(25) Schwarz, M.; Wray, V.; Winterhalter, P. *J. Agric. Food Chem.* **2004**, *52*, 5095–5101.
(26) Hillebrand, S.; Schwarz, M.; Winterhalter, P. *J. Agric. Food Chem.* **2004**, *52*, 7331–7338.
(27) Rein, M. J.; Ollilainen, V.; Vahermo, M.; Yli-Kauhaluoma, J.; Heinonen, M. *Eur. Food Res. Technol.* **2005**, *202*, 239–244.
(28) Marston, A.; Hostettmann, K. In *Flavonoids: Chemistry, Biochemistry and Applications*; Andersen, Ø. M., Markham, K. R., Eds.; Taylor & Francis Group: Oxford, U. K., 2009; Chapter 1, pp 1−32.
(29) Welch, C. R.; Wu, Q.; Simon, J. E. *Curr. Anal. Chem.* **2008**, *4*, 75–101.
(30) Alcade-Eon, C.; Escribano-Baiolon, M. T.; Santos-Buelga, C.; Rivas-Gonzalo, J. C *Anal. Chim. Acta* **2004**, *513*, 305–318.
(31) De Villiers, A.; Vanhoenacker, G.; Majek, P.; Sandra, P. *J. Chromatogr., A* **2004**, *1054*, 195–204.
(32) Alcade-Eon, C.; Escribano-Baiolon, M. T.; Santos-Buelga, C.; Rivas-Gonzalo, J. C *Anal. Chim. Acta* **2004**, *563*, 238–254.
(33) Vergara, C.; Mardones, C.; Hermosín-Gutiérrez, I.; von Baer, D. *J. Chromatogr., A* **2010**, *1217*, 5710–5717.
(34) Giusti, M. M.; Wrolstad, R. E. In *Current Protocols in Food Analytical Chemistry*; Wrolstad, R. E., Ed.; John Wiley & Sons: New York, 2001; No. Unit F1.2.1-13.
(35) Asenstorfer, R. E.; Iland, P. G.; Tate, M. T.; Jones, G. J. *Anal. Biochem.* **2003**, *318*, 291–299.
(36) Torskangerpoll, K.; Børve, K. J.; Andersen, Ø. M.; Leif J. Sæthre, L. J. *Spectrochim. Acta, Part A* **1999**, *55*, 761–771.
(37) Sakata, K.; Saito, N.; Honda, T. *Tetrahedron* **2006**, *62*, 3721–3731.
(38) Woodford, J. N. *Chem. Phys. Lett.* **2005**, *410*, 182–187.
(39) Ferreira da Silva, P.; Lima, J. C.; Freitas, A. A; Shimizu, K.; Maçanita, A. L.; Quina, F. H. *J. Phys. Chem. A* **2005**, *109*, 7329–7338.
(40) Leopoldini, M.; Rondinelli, F.; Russo, N.; Toscano, M. *J. Agric. Food Chem.* **2010**, *58*, 8862–8871.
(41) Estévez, L.; Mosquera, R. A. *J. Phys. Chem. A* **2008**, *112*, 10614–10623.
(42) Carvalho, A. R. F.; Oliveira, J.; de Freitas, V.; Silva, A.; Mateus, N.; Melo, A. *THEOCHEM* **2010**, *946*, 113–118.
(43) Carvalho, A. R. F.; Oliveira, J.; de Freitas, V.; Mateus, N.; Melo, A. *THEOCHEM* **2010**, *948*, 61–64.
(44) Freitas, A. A.; Shimizu, K. ; Dias, L. G.; Quina, F. H. *J. Braz. Chem. Soc.* **2007**, *18*, 1537−1546.
(45) Casida, M. E. *THEOCHEM* **2010**, *914*, 3–18.
(46) Hättig, C.; Weigend, F. *J. Chem. Phys.* **2000**, *113*, 5154–5161.
(47) Ahlrichs, R.; Bär, M.; Häser, M.; Horn, H.; Kölmel, C. *Chem. Phys. Lett.* **1989**, *162*, 165–169.
(48) Perdew, J. P. *Phys. Rev. B* **1986**, *33*, 8822–8824.
(49) Becke, A. D. *Phys. Rev. A* **1988**, *38*, 3098–3100.
(50) Eichkorn, K.; Treutler, O.; Öhm, H.; Häser, M.; Ahlrichs, R. *Chem. Phys. Lett.* **1995**, *242*, 652–660.
(51) Sierka, M.; Hogekamp, A.; Ahlrichs, R. *J. Chem. Phys.* **2003**, *118*, 9136–9148.
(52) Schäfer, A.; Horn, H.; Ahlrichs, R. *J. Chem. Phys.* **1992**, *97*, 2571–2577.
(53) Eichkorn, K.; Weigend, F.; Treutler, O.; Ahlrichs, R. *Theor. Chem. Acc.* **1997**, *97*, 119–124.
(54) Ernzerhof, M.; Scuseria, G. E. *J. Chem. Phys.* **1999**, *110*, 5029–5036.
(55) Perdew, J. P.; Ernzerhof, M.; Burke, K. *J. Chem. Phys.* **1996**, *105*, 9982–9985.
(56) Schäfer, A.; Huber, C.; Ahlrichs, R. *J. Chem. Phys.* **1994**, *100*, 5829–5835.
(57) Dunning, T. H., Jr. *J. Chem. Phys.* **1989**, *90*, 1007–1023.
(58) Quartarolo, A. D.; Sicilia, E.; Russo, N. *J. Chem. Theory Comput.* **2009**, *5*, 1849–1857.
(59) Quartarolo, A. D.; Russo, N.; Sicilia, E.; Lelj, F. *J. Chem. Theory Comput.* **2007**, *3*, 860–869.
(60) Jacquemin, D.; Perpète, E. A.; Ciofini, I.; Adamo, C. *Acc. Chem. Res.* **2009**, *42*, 326–334.
(61) Perpète, E. A.; Jacquemin, D. *THEOCHEM* **2009**, *914*, 100–105.
(62) Klamt, A.; Schuurmann, G. *J. Chem. Soc., Perkin Trans. 2* **1996**, *5*,
799–805.
(63) Klamt, A.; Jonas, V. *J. Chem. Phys.* **1996**, *105*, 9972–9981.
(64) Gorelsky, S. I. *SWizard Program*, revision 4.2; York University: Ontario, Canada, 1998. http://www.sg-chem.net/swizard/ (accessed March 2011).
(65) Hättig, C.; Hellweg, A.; Köhn, A. *Phys. Chem. Chem. Phys.* **2006**, *8*, 1159–1169.
(66) Cramer, J. C.; Truhlar, D. G. *J. Am. Chem. Soc.* **1993**, *115*, 5745–5153.
(67) Molteni, C.; Parrinello, M. *J. Am. Chem. Soc.* **1998**, *120*, 2168–2171.
(68) Mulliken, R. S. *J. Chem. Phys.* **1995**, *23*, 1833–1834.
(69) Mulliken, R. S. *J. Chem. Phys.* **1995**, *23*, 1841–1846.